Appendix I

Understanding the Mechanism of Polyamide Nuclear Localization

*Identification of a target probe and probe inhibition experiments were performed in collaboration with Benjamin S. Edelson; chemical inhibition of cellular uptake was performed in collaboration with Ryan L. Stafford; polyamides **FITC-2**–**FITC-5** were synthesized by Tim P. Best.*

Abstract

Conjugation of fluorescein to the C-terminal end of pyrrole-imidazole polyamides appears to facilitate their cellular uptake and subsequent localization to cell nuclei. This process has been shown to be both temperature- and energy-dependent, indicating an active transport mechanism. We hypothesized that a polyamide-fluorescein conjugate that inhibits this process will do so by binding to proteins that play a key role in the uptake pathway. To identify these cellular proteins, a polyamide-fluorescein uptake inhibitor carrying a photo-activatable diazirine group was synthesized, incubated with target cells, and crosslinked to bound proteins. Successful crosslinking was confirmed by Western blot, but subsequent attempts to identify these proteins by mass spectrometry were unsuccessful due to the presence of high levels of contaminants. Efforts to gain further insights into the mechanisms of the cellular and nuclear uptake of polyamides using a panel of inhibitory conditions and confocal microscopy have demonstrated the need for a quantitative assay of the nuclear localization of polyamides.

Introduction

With their demonstrated ability to bind to predetermined DNA sequences at comparable affinities to those of naturally occurring DNA-binding proteins (1,2), pyrrole-imidazole polyamides have great potential as tools in molecular biology and human medicine. Their efficacy in these roles requires that they be able to: 1) permeate the plasma membrane and 2) access the nuclei of living cells. This has proven to be a continuing challenge in exploiting these molecules. A more complete understanding of the molecular mechanisms involved in the import of polyamides into living cells would greatly improve our ability to rationally design functional polyamides for use in both research and medicinal applications.

Prior work has addressed the issue of the cellular uptake and nuclear localization of polyamides by conjugating polyamides to fluorophores and visualizing their localization in live cells using confocal microscopy (3–6). In addition, recent studies have used quantitative real-time RT-PCR as an assay for cellular uptake and have verified the nuclear uptake of polyamides that are not conjugated to fluorophores (7).

Best et al. studied the molecular determinants of the nuclear localization of polyamide-fluorophore conjugates in 13 cultured cell lines, looking at how factors such as the identity of the fluorophore, structure, and molecular weight influence nuclear localization properties (3,4). Although some general trends were identified, the prediction of the cellular localization properties of a given polyamide or polyamide-fluorophore conjugate *a priori* is still not possible. Instead, the localization of polyamides must be determined experimentally for each molecule.

We would like to understand the mechanisms by which polyamides both permeate the plasma membrane and access the cell nucleus. This knowledge would give us insights that could potentially allow the rational design of polyamides with known uptake properties. These results may also have implications for the cellular and nuclear uptake of other small molecules.

Previous experiments have provided some insights into the mechanism of nuclear uptake of polyamides. In experiments conducted by Best et al., it was found that a polyamide-fluorescein conjugate that normally localizes to the nuclei of live HeLa cells could be inhibited if the HeLa cells were first incubated in an energy-inhibiting media (4). When the cells were subsequently washed and incubated with normal media, the nuclear localization of the polyamide was rescued. Nuclear localization was also found to be temperature-dependent (8). These data led us to conclude that polyamide-fluorescein conjugates are taken up by cells through an active transport pathway, possibly involving a membrane transport protein.

We hypothesized that if a polyamide could be found that inhibited the nuclear localization of another polyamide, then the inhibition may occur via binding to a protein involved in the uptake pathway. Conjugating the inhibitory polyamide to a photo-activatable group would allow us to use the inhibitory polyamide as a probe to pull down key proteins involved in the uptake pathway. Antibodies to fluorescein are commercially available, providing a simple means to pull down the captured proteins. Once isolated, the captured proteins could be identified by liquid chromatography and tandem mass spectrometry (LC-MS/MS).

Results and Discussion

Design and Synthesis of the Probe

In identifying a target molecule to serve as the probe, we considered many factors, including polyamide sequence, the identity and point of attachment of the photo-activatable group, and the point of attachment of the fluorescein moiety. To address these issues, we hypothesized that an inhibitor would be more likely to act by binding to a protein involved in the uptake pathway if its structure differed only slightly from that of a polyamide which localizes to the cell nucleus but which itself was excluded from cells. We also sought a molecule with easy synthetic access since relatively large quantities of the probe would be required.

It was essential for the probe to inhibit another polyamide from localizing to the nuclei of live cells. Using confocal microscopy, Ben Edelson screened a library of 15 polyamide-fluorescein conjugates known to be excluded from live HeLa cells for their ability to inhibit the nuclear uptake of polyamide conjugate **TMR-1**, previously shown to localize to the nuclei of live HeLa cells (data not shown). Conjugate **TMR-1** was chosen for this assay because its non-overlapping tetramethylrhodamine dye allowed for easy differentiation from the polyamide-fluorescein conjugates during microscopy. FITC conjugates **FITC2**–**FITC-5** were found to be the best nuclear uptake inhibitors (Figure I.1).

Polyamide conjugate **FITC-2** was selected as the parent molecule for the target probe because its acetylated $^{AcHN}\gamma$-turn could be easily substituted with the desired photo-activatable group and because its core ring sequence consisted of the standard pyrrole and imidazole rings. A beta-alanine residue was appended to the C-terminal end

of the target molecule's core sequence since it has been found to generally be a negative determinant for polyamide nuclear access. In addition, the beta-alanine allowed us to synthesize the probe on the robust phenylacetamidomethyl (PAM) resin, giving us easy access to large quantities of the target molecule.

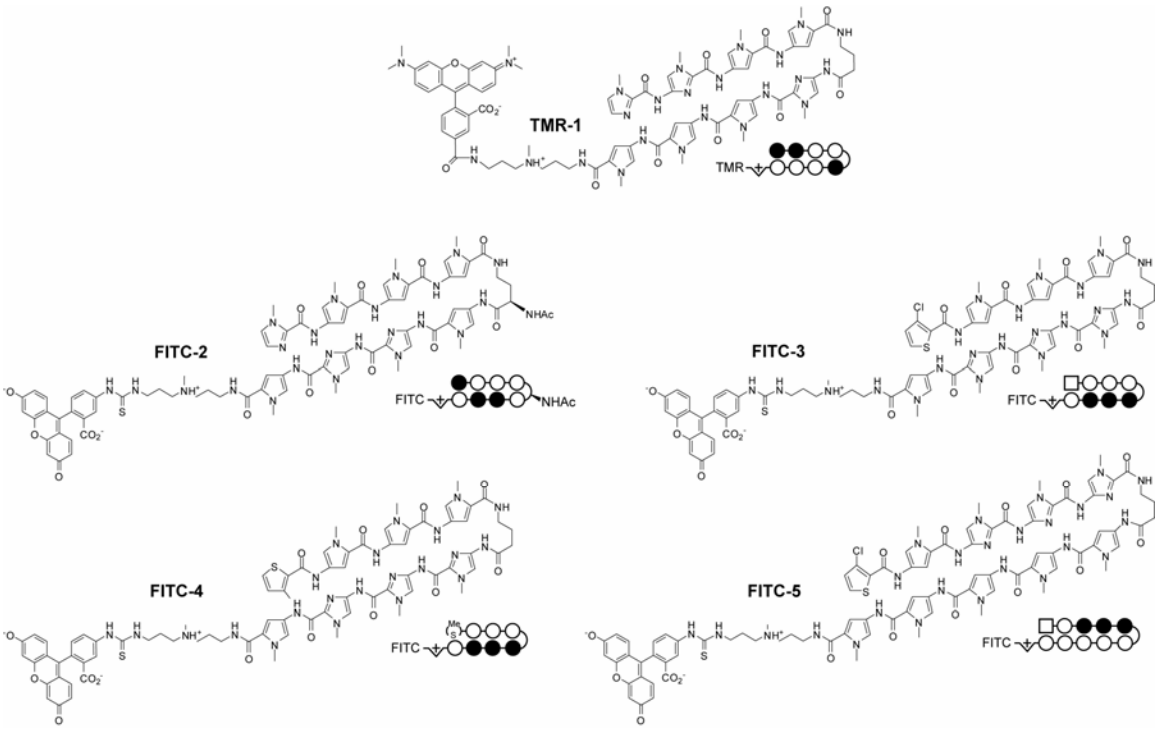

Figure I.1. Chemical and ball-and-stick structures of tetramethylrhodamine-polyamide conjugate **TMR-1**, which normally localizes to the nuclei of HeLa cells, and of fluorescein-polyamide conjugates **FITC-2**–**FITC-5**, which were found to be the best inhibitors of the nuclear uptake of conjugate **TMR-1**

The (trifluoromethyl)aryldiazirine moiety (molecule **6**) was chosen as the photo-activatable group for a number of reasons, including its small size, relatively long wavelength of activation, and stability in the dark (9,10). Photolysis of the (trifluoromethyl)aryldiazirine group by light of a wavelength around 353 nm gives the corresponding singlet carbene (10), a highly reactive intermediate capable even of C-H

bond insertion. In addition, its commercial availability as the benzoic acid derivative provided easy synthetic access.

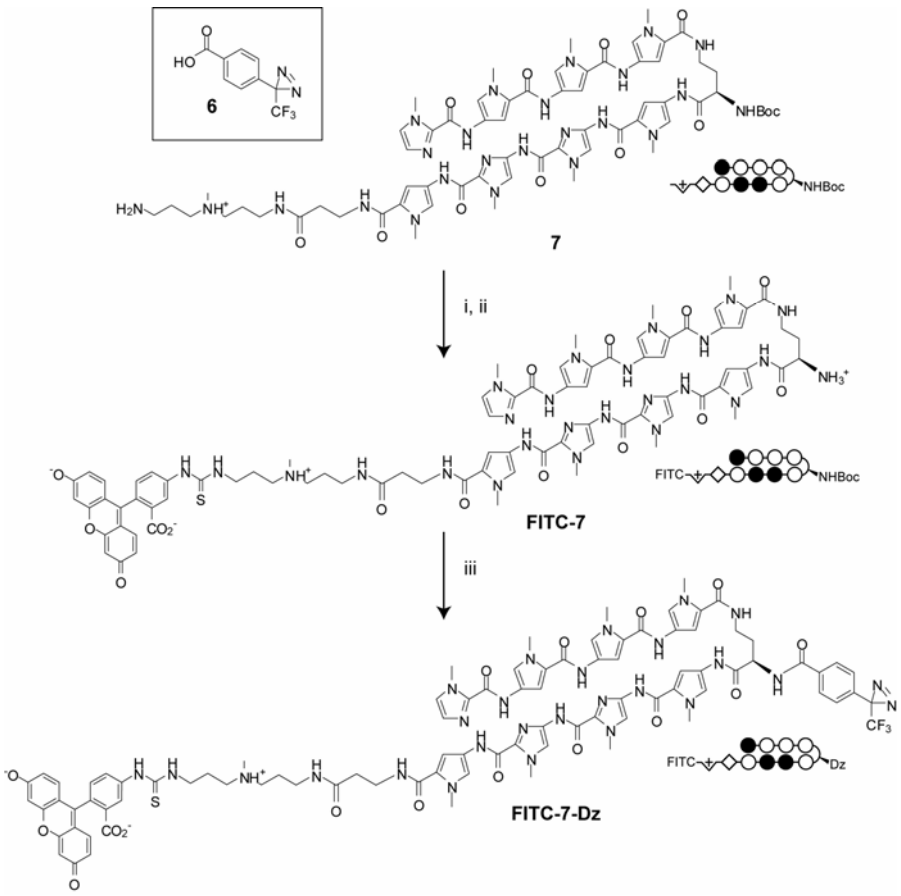

Scheme I.1. Synthesis of the polyamide probe **FITC-7-Dz**. i) fluorescein-5-isothiocyanate, DIEA, DMF; ii) trifluoroacetic acid, triethylsilane; iii) DCC/HOBt-activated **6**, DIEA, DMF

With these considerations in mind, polyamide conjugate **FITC-7-Dz** was selected as the target probe (Scheme I.1). Parent polyamide **7** was synthesized according to standard solid-phase protocols (11) on β-Ala-Pam resin followed by cleavage from resin with 3,3'-diamino-N-methyl-dipropylamine and purification by reverse-phase high-performance liquid chromatography (HPLC). Parent molecule **7** was treated with fluorescein-5-isothiocyanate (5-FITC) and *N, N*-diisopropylethylamine (DIEA) in *N, N*-

dimethylformamide (DMF) followed by Boc deprotection with trifluoroacetic acid (TFA) and triethylsilane, yielding the polyamide-fluorescein conjugate **FITC-7**. The α-amino group on the $^{H_2N}\gamma$-turn of compound **FITC-7** was then coupled to the activated carboxylate derivative of 4-(1-azi-2,2,2-trifluoroethyl)benzoic acid (**6**) using standard dicylcohexylcarbodiimide/1-hydroxybenzotriazole hydrate (DCC/HOBt) conditions to yield the final target compound **FITC-7-Dz**. It should be noted that verification of the mass of the final product was performed using electrospray ionization mass spectrometry (ESI-MS) rather than matrix-assisted laser desorption/ionization-time of flight (MALDI-TOF) mass spectrometry, as is normally used for polyamide synthesis. This was necessitated by the fact that the MALDI-TOF laser emits at a wavelength that activates the diazirine moiety.

Inhibition by the Probe

Before using the probe to capture proteins, we first wanted to verify using confocal microscopy that the probe could indeed inhibit polyamide nuclear localization. As before, we tested the inhibitory properties of the probe in three human cell lines — PC3, HeLa, and MCF-7 (Figure I.2). These cell lines were chosen because they are the three most permissive with regards to polyamide nuclear localization (3,4), which we hypothesized would correlate to levels of protein related to the uptake pathway. These experiments verified the inhibitory properties of probe polyamide **FITC-7-Dz** and, furthermore, that the probe was excluded from the three cell lines.

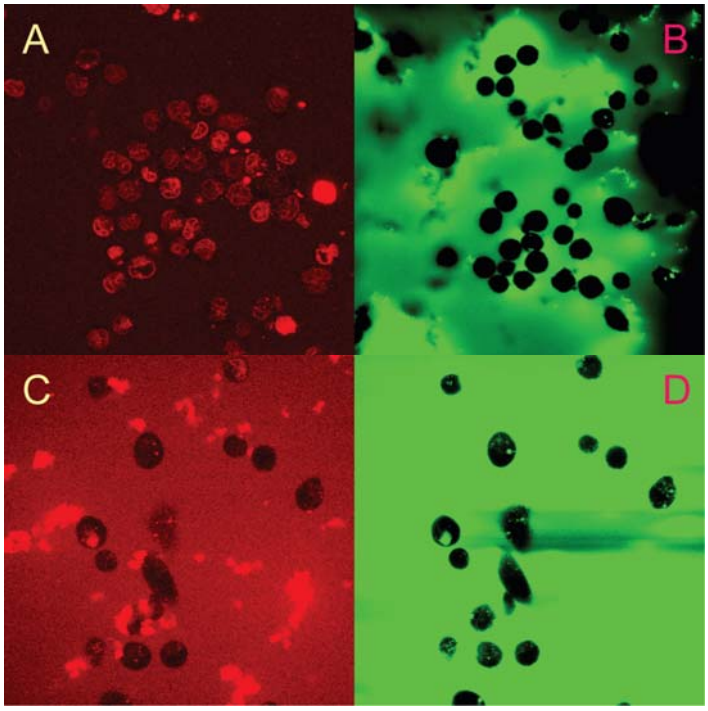

Figure I.2. Representative confocal microscopy data demonstrating the inhibition of the nuclear localization of conjugate **TMR-1** by probe **FITC-7-Dz**. Images shown in green were obtained using the standard filter sets for fluorescein. Images shown in red were obtained with the standard filter sets for tetramethylrhodamine. Images C and D are the same plate imaged by sequential excitation. 24 h after plating, PC3 cells were treated either with probe **FITC-7-Dz** (**B**–**D**; 5 μM final concentration) or DMSO control (**A**). 14 hrs after the addition of **FITC-7-Dz**, conjugate **TMR-1** was added (**A**, **C**–**D**; 2 μM final concentration) or DMSO control (**B**). The cells were imaged 12 hrs after the addition of **TMR-1**.

Optimization of Irradiation Conditions

To determine the optimal light source and length of irradiation time, a time-course experiment was performed using probe **FITC-7-Dz** (Figure I.3). In addition, its benzoic acid derivative **FITC-7-Bz** was synthesized as a control. Irradiation using a photoreactor (λ = 350 nm) was compared to that using the more convenient handheld UV lamp (λ = 365 nm). Photo-activation appeared greater when reaction was performed with the photoreactor. In addition, after 10 min of irradiation, photoreaction appeared to plateau while polyamide degradation continued to increase. Thus, 10 min was selected as the optimal length of time for irradiation of samples.

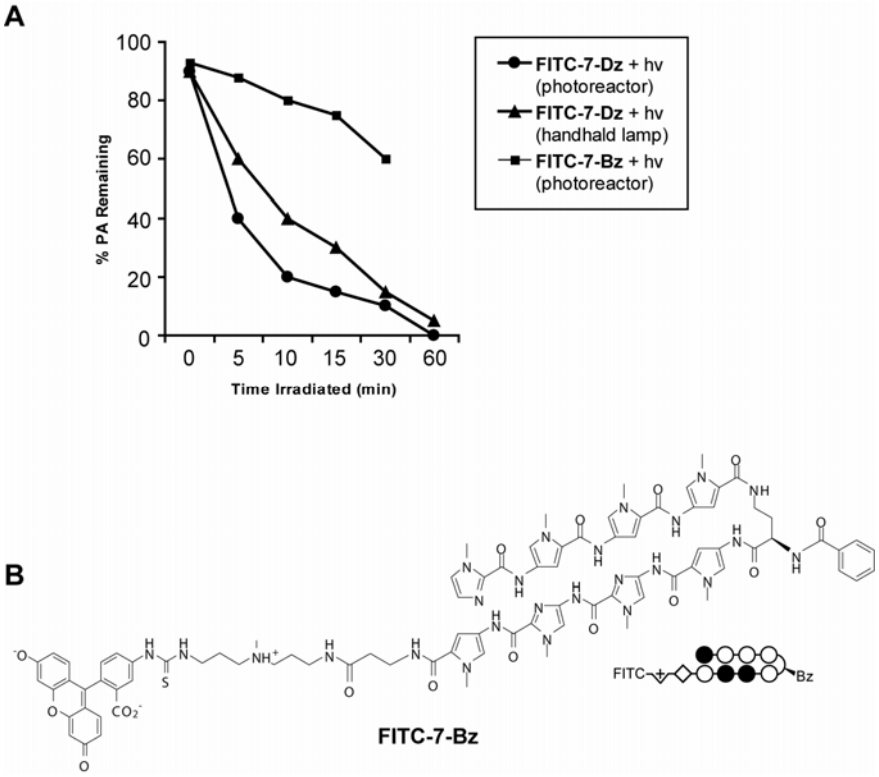

Figure I.3. (**A**) Optimization of irradiation conditions for diazirine activation of probe **FITC-7-Dz**. A stock solution of conjugate was irradiated, and aliquots were removed at regular intervals and assayed by analytical HPLC. (**B**) Structure of the control polyamide-benzoic acid conjugate **FITC-7-Bz**.

Protein Capture, Isolation, and Identification

With a confirmed inhibitory polyamide probe in hand, we proceeded to capture, isolate, and identify proteins with the probe. Briefly, we first incubated the cells with the probe for 12–15 hrs. Upon irradiation of the mixture, the diazirine moiety was activated and covalently bound to its cellular partner proteins. The cells were then harvested, lysed in boiling 1% SDS, and sonicated. These harsh conditions were necessary to ensure the solubility of all membrane proteins, as we anticipated a membrane protein would be involved in the transport process. The cell lysate was then purified via anti-fluorescein affinity chromatography. The combined elution fractions were digested with trypsin, and

the resulting peptides were analyzed by mass spectrometry. Using commercially available fluorescein-conjugated bovine serum albumin as a control molecule, each of these procedures was successfully performed and optimized (data not shown).

Experiments with PC3 cells, a human prostate cancer cell line, demonstrated the probe was capable of successfully conjugating cellular proteins (Figure I.4). We found that an essential component of the protocol was the use of a photoreactor equipped with eight 8W UVA light bulbs irradiating at 350 nm to photo-activate the probe. In order to identify whether these proteins were involved in cellular trafficking, we proceeded to identify these target proteins.

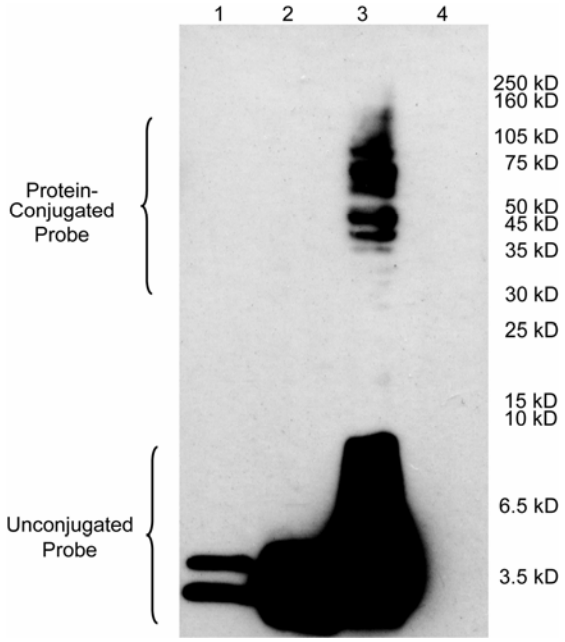

Figure I.4. Successful conjugation of probe **FITC-7-Dz** to proteins in live PC3 cells. PC3 and HeLa cells were incubated with probe **FITC-7-Dz** (5 μM) or DMSO control, irradiated at 350 nm in a photoreactor for 10 min, and lysed. Lane 1: 65 pmol of probe **FITC-7-Dz** irradiated at 350 nm for 10 min without cells. Lane 2: Lysate from probe **FITC-7-Dz**-treated HeLa cells (75 μg total protein). Lane 3: Lysate from probe **FITC-7-Dz**-treated PC3 cells (75 μg total protein). Lane 4: Lysate from untreated control PC3 cells (75 μg total protein). Proteins were visualized by Western blot using an anti-fluorescein antibody.

Further experiments also indicated that the high levels of two contaminants — polyethylene glycol (PEG) from the antibody column and probe unconjugated to protein

— would be challenges that would need to be addressed (Figure I.5). In particular, if unremoved, the mass spectrometry signal of any desired peptide peaks would potentially be undetectable due to the strong signals originating from the two contaminating molecules. Furthermore, unconjugated probe in the cell lysate mixture would saturate available binding sites in the antibody column, preventing the desired protein-conjugated probe from being isolated.

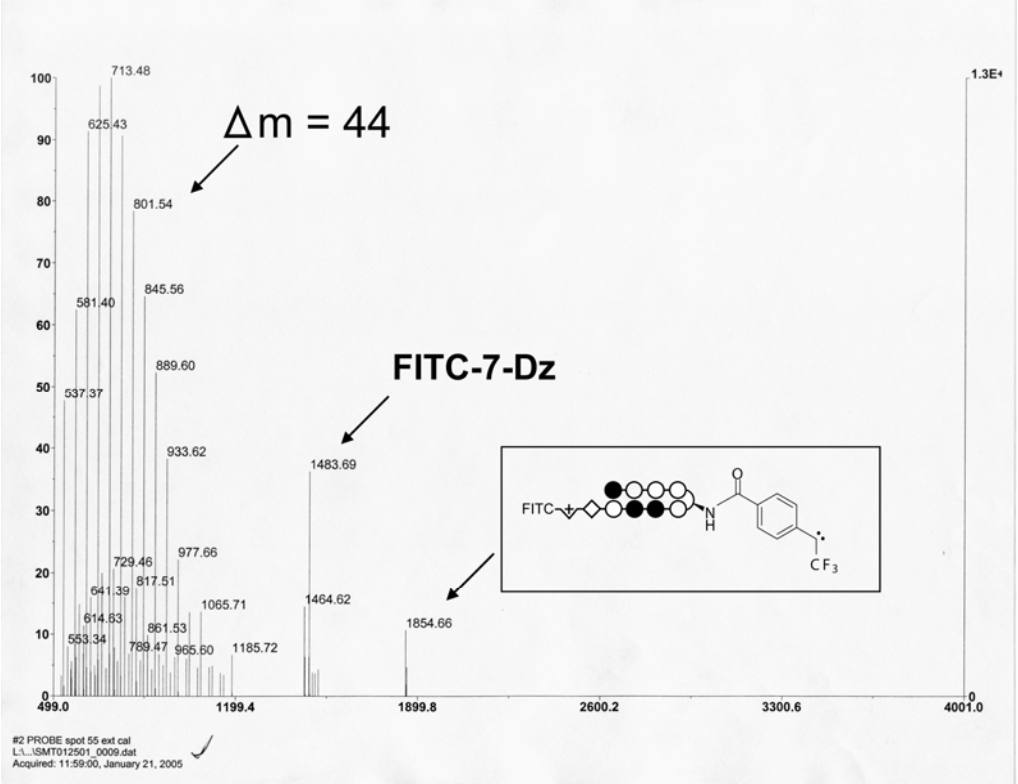

Figure I.5. Mass spectral analysis of purified PC3 cell lysate. PC3 cells were incubated with probe **FITC-7-Dz** (5 μM), irradiated, and lysed. The cell lysate was purified over an anti-fluorescein antibody column, and the elution fractions were combined, trypsin-digested, purified with a mini C-18 spin column, and analyzed by MALDI-TOF MS. The set of peaks with a mass difference of 44 amu corresponds to polyethylene glycol. MALDI-TOF data was collected with Dr. Mona Shahgholi.

We carried out a large-scale experiment addressing these issues. To remove unconjugated probe from the cell lysate, the lysate was dialyzed extensively. Flow-

through lysate was recycled multiple times over the anti-fluorescein antibody column to increase protein yield. In an attempt to remove PEG contamination, the combined elution fractions were concentrated via ultrafiltration. As recommended by the manufacturer to minimize protein loss, the ultrafiltration devices were blocked with milk followed by extensive washing. Subsequent MALDI-TOF mass spectrometry of the concentrated samples showed this step was unsuccessful in removing the PEG contamination. Thus, the lysate was purified by polyacrylamide gel electrophoresis (PAGE) followed by visualization with silver stain (Figure I.6), a step that removes the PEG but decreases protein yield. The gel was run very briefly (approximately 2 cm) to minimize the amount of gel submitted for analysis, as increasing the amount of gel would decrease the final sensitivity. Bands from the silver stained gel, as diagrammed in Figure I.6, were excised and submitted to the Caltech Protein/Peptide MicroAnalytical Laboratory (PPMAL) for trypsin digestion and LC-MS/MS analysis.

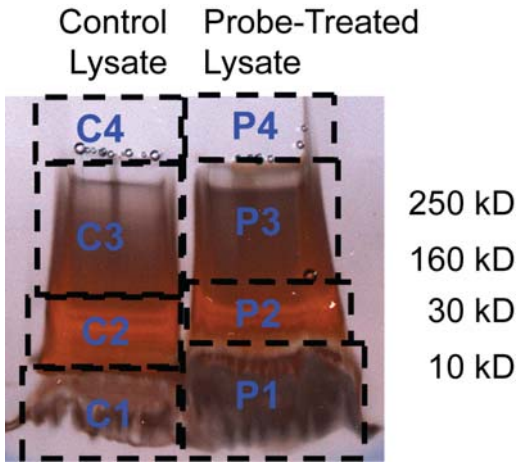

Figure I.6. PAGE purification of PC3 cell lysate. Lysate from PC3 cells incubated with probe **FITC-7-Dz** (5 μM) or DMSO control were irradiated and lysed. The cell lysate was dialyzed and purified over an anti-fluorescein antibody column. The elution fractions were combined, concentrated by ultrafiltration, and run briefly on a 4–12% polyacrylamide gel. Proteins were visualized by silver staining. Bands were excised as indicated and submitted for trypsin digestion and LC-MS/MS analysis.

The results obtained by the PPMAL are summarized in Table I.1. Virtually all of the proteins identified were obvious contaminants: keratins from skin and hair during handling of the samples, milk proteins from the ultrafiltration devices, antibodies from the antibody column, and trypsin from the trypsin digestion. Actin was the most common non-contaminating protein identified, probably due to the high levels at which it is expressed in cells (12). Its presence in the control sample indicates non-specific interactions between actin and the anti-fluorescein antibody column. The only protein identified in the probe-treated cells that was not also identified in the untreated cells was the protein dihydrofolate reductase (DHFR). DHFR is a cytoplasmic protein that synthesizes tetrahydrofolate from 7,8-dihydrofolate, a key step in the biosynthesis of DNA (13). Given its known function, it is unlikely that DHFR is involved in the polyamide uptake pathway and its identification is likely due to non-specific interactions with the anti-fluorescein antibody column or the probe.

Excised Bands	**Proteins Identified from Control Lysate**	**Proteins Identified from Probe Lysate**
C1/P1	caseins, lactoglobulins, keratins, antibody chains, actins, human elongation factor -1-delta, histone H2A.2	caseins, lactoglobulins, keratins, antibody chains, actins
C2/P2	casein, lactoferrin, antibody chains	casein, keratins, antibody chains, trypsin precursor
C3/P3	casein, lactoferrin, keratin	casein, lactoferrin, dihydrofolate reductase
C4/P4	casein, lactoferrin, keratin	casein, keratins, cytokeratins, histone 2H3C

Table I.1. Summary of proteins identified from the excised gel bands, as shown in Figure I.6. The gel bands were digested with trypsin and the resulting peptides analyzed by LC-MS/MS by the Caltech Protein/Peptide MicroAnalytical Laboratory (PPMAL). Only statistically significant hits are reported. Protein identification was considered statistically significant if its probability based Mowse score was greater than 50.

A New Approach to Understanding the Nuclear Localization of Polyamides

Based on the challenges encountered with the approach, we decided to reassess our hypothesis and methodology. First, we wanted to more firmly establish the energy and temperature dependence of the nuclear uptake of polyamides through a series of experiments. Specifically, we investigated a wider temperature range and a broader panel of energy inhibitors that work through a variety of mechanisms. We also tested a panel of drugs for their ability to influence polyamide nuclear uptake. In particular, endocytosis is a temperature- and energy-dependent mechanism commonly employed by cells to transport molecules across their plasma membranes, and a number of drugs are known to inhibit this process at a variety of stages.

As in the previous studies, we decided to assay uptake inhibition with confocal microscopy. We examined the properties of polyamide conjugate **FITC-1** (Figure I.7) because it was the polyamide used in the energy inhibition studies performed by Best et al. and because it is well-established as a polyamide that readily localizes to the nuclei of many cell lines (4).

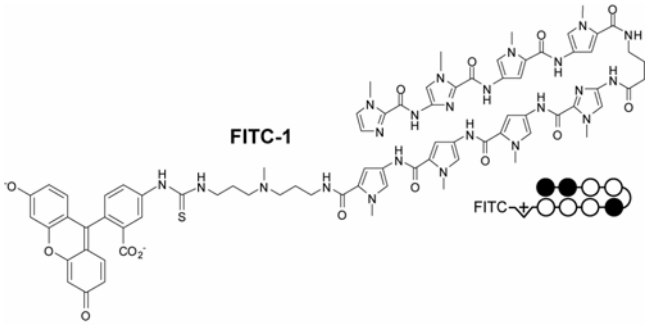

Figure I.7. Chemical and ball-and-stick structure of polyamide **FITC-1**, a polyamide conjugate previously established to localize readily to the nuclei of many cell lines

We chose two control molecules with known uptake mechanisms to test our ability to observe inhibition with microscopy. Tetramethylrhodamine-conjugated

transferrin — a protein known to enter cells through an endocytic pathway (14) and used successfully as a control molecule in similar studies (15) — was selected as a positive control molecule.

Conditions Tested	Effect of Inhibitor(s)*	FITC-1	TMR-Tf	Hoechst
4 ^{o}C in normal media	--	Complete Inhibition	Complete Inhibition	No Inhibition
26 ^{o}C in normal media	--	Partial Inhibition	Partial Inhibition	No Inhibition
4 h at 4 ^{o}C in normal media, then 2 h at 37 ^{o}C	--	Uptake Rescued	Partial Uptake Rescued	No Change
sodium pyruvate- and Glc-free media	--	No Inhibition	Partial Inhibition?	No Inhibition
6 mM dGlc, 10 mM NaN_3 in Na pyruvate- and Glc-free media	induces ATP depletion	Complete Inhibition	Complete Inhibition	No Inhibition
20 μM/100 μM rotenone in Na pyruvate- and Glc-free media	inhibits mitochondrial electron transport	Increased Uptake?	No Inhibition?	--
1 mM/2mM KCN in sodium pyruvate- and Glc-free media	inhibits cytochrome oxidase	No Inhibition?	No Inhibition?	--
200 μM DNP, 1mM NaF/1 mM DNP, 2 mM NaF in Na pyruvate- and Glc-free media	inhibits oxidative phosphorylation (DNP) and glycolysis (NaF)	No Inhibition?	Partial Inhibition?	--
0.5 M sucrose in normal media	inhibits clathrin-coated pit formation	Partial Inhibition?	Partial Inhibition	--
50 μM chloroquine in normal media	inhibits acidification of endocytic vesicles	Increased Uptake?	Increased Uptake?	--
30 μM chloropromazine in normal media	inhibits clathrin-coated pit-mediated endocytosis	No Inhibition?	No Inhibition?	--

Table I.2. Results for HeLa cells treated with a panel of inhibitory conditions to study their effects on the nuclear localization of conjugate **FITC-1**, the cellular uptake of tetramethylrhodamine-conjugated transferrin (TMR-Tf), or the nuclear localization of Hoechst 33342. Unless otherwise stated, HeLa cells were incubated in the solution stated for 30 min at 37 ^{o}C. The given fluorophore/fluorophore conjugate was then added, and the cells were allowed to incubate at 37 ^{o}C for an additional 4 hrs prior to imaging by confocal microscopy with the appropriate filters. Results performed in normal media are compared to cells incubated with normal media (DMEM) at 37 ^{o}C. For studies using sodium pyruvate- and glucose-free media (DMEM), results were compared to cells incubated with the sodium pyruvate- and glucose-free media. A "?" indicates equivocal data. dGlc = dideoxyglucose; DNP = 2,4-dinitrophenol. * Described in references (15–19)

As a control molecule known to diffuse through cell membranes passively, we chose Hoechst 33342 (20). Hoechst only fluoresces upon binding to DNA in cell nuclei (20), making it a non-ideal control molecule. However, we found few molecules that would fluoresce in a non-overlapping region of the spectrum that had been shown to passively diffuse into cells.

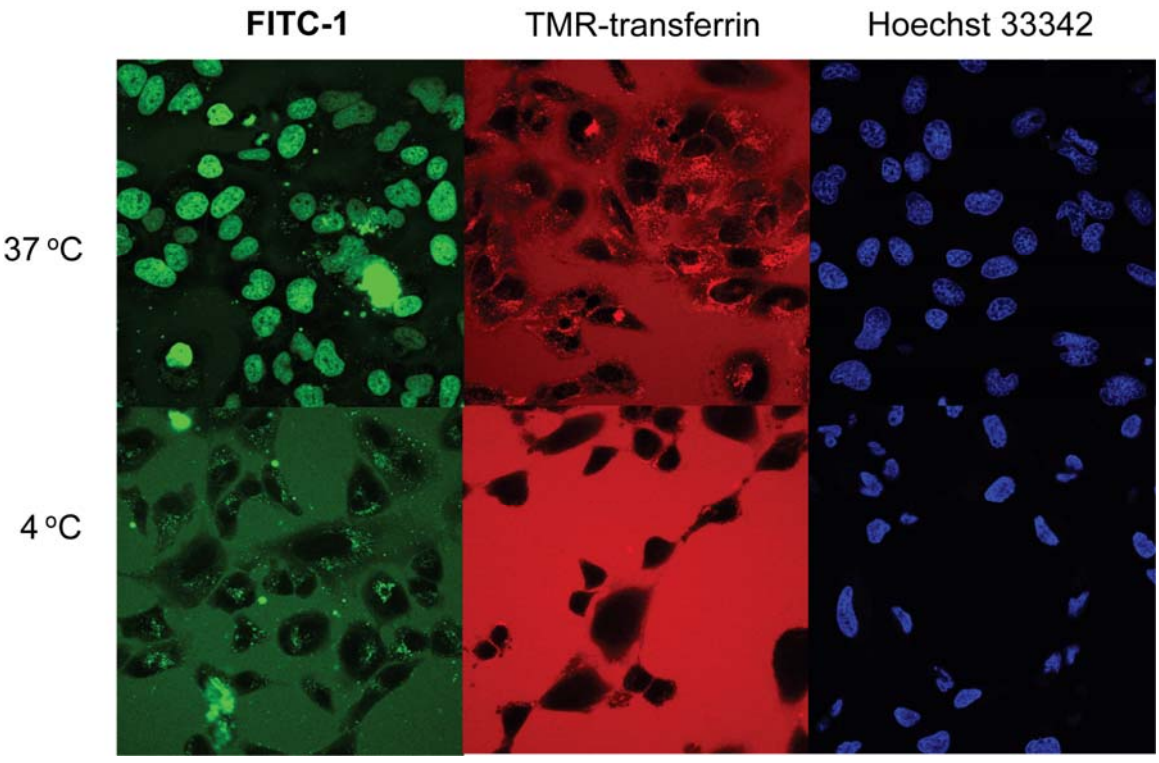

Figure I.8. Temperature dependence of the nuclear localization of conjugate **FITC-1**. HeLa cells were incubated in normal Dubelco's Modified Eagle Medium (DMEM) for 10 min at either 4 °C or 37 °C. The media was exchanged for a media solution containing either **FITC-1** (5 μM), tetramethylrhodamine-conjugated transferrin (1 μM), or Hoechst 33342 (5 μM), and the cells allowed to incubate at 4 °C or 37 °C for an additional 4 h. The cells were then imaged by confocal microscopy using the standard filter settings for the given fluorophore.

Table I.2 summarizes some of the results from these studies, conducted with Ryan Stafford. We successfully reproduced the energy inhibition data obtained by Best et al.

and showed that there is a dramatic inhibition of uptake at temperatures as low as 4 ^{o}C. (Representative data shown in Figure I.8.) However, many of the experiments summarized in Table I.2 resulted in ambiguous data even with our control molecules. Energy inhibitors other than the sodium azide/dideoxyglucose combination tested by Best et al. failed to have the same dramatic inhibition of uptake. We concluded from these preliminary studies that only complete inhibition can be decisively determined from our microscopy assay. The assay did not give us the sensitivity we needed to measure the extent of partial inhibition. In particular, we would like to determine if there is a concentration dependence of uptake with the various inhibitors. A quantitative measurement of uptake will be developed to obtain conclusive results.

Conclusion

A polyamide-diazirine conjugate was successfully synthesized for the capture of proteins involved in the nuclear uptake of polyamides. Target proteins were identified via Western blot, but attempts to isolate and identify these proteins were unsuccessful, probably due to the high levels of contaminants and the low levels of target proteins. Preliminary experiments using confocal microscopy were conducted to investigate polyamide nuclear uptake with a panel of inhibitory conditions. The temperature dependence of uptake was confirmed, and there is data that indicates that uptake is energy-dependent.

Our follow-up studies have not yet conclusively demonstrated whether the mechanism of the nuclear localization of polyamides is an active or passive process. To address this issue, we will develop a quantitative assay for the uptake of polyamides.

Utilization of fluorescence-activated cell sorting (FACS) or fluorescence measurements of cell lysates may provide us with the ability to study the drug concentration dependence of uptake inhibition. Confocal microscopy may still be employed to determine the cellular localization of fluorescence since polyamides can be taken up by cells and trapped in vesicles rather than localizing to the cell nucleus (4). The results from a quantitative assay would give us new insights into the mechanism of polyamide nuclear localization.

In addition, the synthetic methodology developed in these studies can be expanded to other polyamides. Polyamides containing the photolabile diazirine group have the potential to identify *in vivo* polyamide binding partners. To this end, the polyamide-fluorescein-diazirine conjugate **FITC-1-Dz** has been synthesized and found to have some nuclear localization properties in MCF-7 and HeLa cells (Figure I.9). In addition, diazirine conjugates may serve as sequence-specific DNA alkylating agents containing a spatiotemporal switch. However, the binding affinity of a polyamide-diazirine conjugate of structure ImImβIm-$(R)^{Dz}$γ-PyPyPyPy-βDp was found to have a 100-fold decreased binding affinity to its targeted match site relative to its parent polyamide (data not shown).

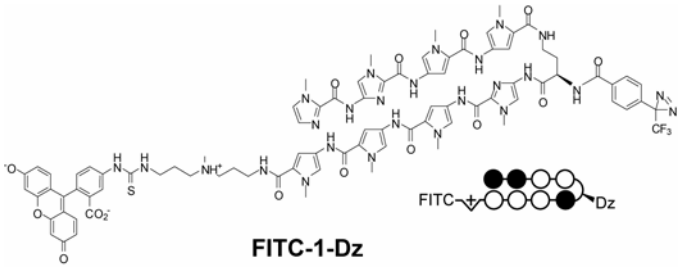

Figure I.9. Chemical and ball-and-stick structure of **FITC-1-Dz**, a polyamide-fluorescein-diazirine conjugate found to be capable of localizing to the nuclei of live cells

Materials and Methods

Synthesis of Polyamides

Polyamide **7** and the parent polyamide of **TMR-1** were synthesized in stepwise fashion on Boc-β-Ala-Pam resin following standard Boc-based solid-phase methods as previously described (11). The polyamides were cleaved by treatment with 70% 3,3'-diamino-*N*-methyldiproplyamine in DMF, heated (37 ^{o}C, 48 h), and purified by preparatory reverse-phase HPLC. Polyamides were recovered as a white powder upon lyophilization of the appropriate fraction.

Polyamides **FITC-7** and **FITC-1** were synthesized from their parents by reaction with fluorescein-5-isothiocyanate (4 equiv.) and DIEA (50 equiv.) in DMF for 2 h at 37 ^{o}C followed by ether precipitation and reaction in 5% triethylsilane in TFA for 30 min at r.t. Following purification by preparatory HPLC, the polyamides were recovered as an orange solid.

Polyamide probe **FITC-7-Dz** was synthesized from conjugate **FITC-7** by reaction in DMF with DIEA (50 eq) and pre-activated 4-(1-azi-2,2,2-trifluoroethyl)benzoic acid (5 eq **6**, 5 eq HOBt, 5 eq DCC in DMF; shaken at 37 ^{o}C for 3 h) for 3 h at 37 ^{o}C. 0.1% TFA in water was added to the reaction mixture, the mixture was purified by prep reverse-phase HPLC, and the final product was recovered as an orange solid upon lyophilization of the appropriate fraction. Benzoic acid conjugate **FITC-7-Bz** was synthesized from polyamide **FITC-7** by similar reaction using pre-activated benzoic acid.

The molecular weights of the diazirine conjugates were verified by ESI MS to avoid excitation of the diazirine moiety by the MALDI laser. For **FITC-7-Bz**, the presence of the fluorescein moiety was verified by UV-Visible spectroscopy and analytical HPLC, and the molecular weight minus FITC was measured by MALDI-TOF MS, as the MALDI laser readily fragments the FITC-polyamide bond. The molecular weights of all other molecules were directly verified by either ESI MS or MALDI-TOF MS, as indicated.

TMR-1: ImImPyPy-γ-ImPyPyPy-Da-TMR MALDI-TOF MS calculated for $C_{81}H_{91}N_{24}O_{13}$ $[M+H]^+$: 1607.72; found: 1607.67

FITC-7-Dz: ImPyPyPy-(*R*)^{Dz}γ-PyImImPy-βDa-FITC ESI MS calculated for $C_{89}H_{92}F_3N_{27}O_{16}S$ $[M+H]^+$: 1882.90; found: 1883.0

FITC-7-Bz: ImPyPyPy-(*R*)^{Bz}γ-PyImImPy-βDa-FITC MALDI-TOF MS calculated for $C_{66}H_{80}N_{24}O_{11}$ $[M\text{-FITC}+H]^+$: 1385.64; found: 1385.57

FITC-1: ImImPyPy-γ-ImPyPyPy-Da-FITC ESI MS calculated for $C_{77}H_{81}N_{23}O_{14}S$ $[M+H]^+$: 1583.6; found: 1584.1

FITC-1-Dz: ImImPyPy-(*R*)^{Dz}γ-ImPyPyPy-Da-FITC ESI MS calculated for $C_{86}H_{85}F_3N_{26}O_{15}S$ $[M+H]^+$: 1811.64; found: 1811.8

Irradiation of Samples

Irradiation was performed on solutions contained in open Petri dishes. Dishes were inside a Luzchem photobox fitted with eight 8 W bulbs irradiating 350 nm light, or a handheld UV lamp was rested directly on top of a dish. For time course experiments, a

stock solution of polyamide or conjugate was prepared such that a 1x solution would give a measurable peak by analytical HPLC. At various time points, 100 μL samples were removed from the irradiated stock solution and assayed for purity by reverse-phase analytical HPLC.

Cell Cultures

The human cancer cell lines MCF-7 and PC3 were cultured in a 5% CO_2 atmosphere at 37 ^{o}C in RPMI medium 1640 supplemented with 10% fetal bovine serum and 1% penicillin/streptomycin. The human cancer cell line HeLa was cultured in a 5% CO_2 atmosphere at 37 ^{o}C in DMEM supplemented with 10% fetal bovine serum and 1% penicillin/streptomycin. All cell lines were purchased from the ATCC.

Determination of the Uptake Inhibition Properties of FITC-7-Dz

Cells were trypsinized for 5 min at 37 ^{o}C, centrifuged for 5 min at 10 ^{o}C at 1500 rpm, and resuspended in fresh media. The cells were plated on culture dishes equipped with glass bottoms for direct imaging at a concentration of 10,000 cells/plate in 150 μL of media. Cells were grown for 24 h. The media was then removed and replaced with 142.5 μL of fresh media and 7.5 μL of a 100 μM solution of probe **FITC-7-Dz** dissolved in 20% DMSO/H_2O. Control cells were treated with a 7.5 μL solution of 20% DMSO/H_2O. The cells were incubated an additional 14 h, upon which 3 μL of a 100 μM solution of polyamide **TMR-1** was added with enough media to give a total volume of 150 μL. Control cells did not receive polyamide **TMR-1.** Cells were imaged after an

additional 10 h of incubation. Imaging was performed with a X40 oil-immersion objective lens on a Zeiss LSM 5 Pascal inverted laser scanning microscope.

Protein Capture

Cells were plated on 100x20 mm tissue culture plates (Sarstedt) at 2 million cells/plate and allowed to grow for 24 h. To each plate, the media was replaced with 12 mL of fresh media containing probe **FITC-7-Dz** at a final concentration of 5 μM. The cells were incubated a further 12–15 h after which time each plate was placed in a photoreactor (Luzchem; 8 8 W UVA light bulbs irradiating at 350 nm) and irradiated for 10 min. The media from each plate was then removed and the plates washed with 5 mL of Hanks' Buffered Salt Solution (HBSS). The cells were trypsinzed in 3 mL of trypsin for 5 min at 37 ^{o}C, and centrifuged at 1500 rpm for 5 min at 10 ^{o}C. The combined cell pellet was lysed in a minimal volume of boiling 1% SDS containing protease inhibitors (Roche mini protease inhibitor cocktail tablet). The pellet was then sonicated at 40 mA for 5 x 1 sec, pulsed setting. The lysate was then boiled for 5 min and its protein concentration determined using the BCA assay (Pierce).

Western Blotting

Western blots were performed based on manufacturer protocols (Invitrogen). Briefly, samples were run at 200 V on 4–12% Bis-Tris gels using either MOPS or MES buffer. Following polyacrylamide gel electrophoresis, proteins were transferred to PVDF membrane (Invitrogen) for 1 h at 30 V. The blot was then incubated in a blocking solution (5% milk + 0.05% Tween) for 1 h at r.t., then probed for 1 h with 1:5000

polyclonal affinity-purified anti-fluorescein goat antibody solution (Rockland International), washed with a PBS + Tween solution, incubated with a 1:5000 horse radish peroxidase-conjugated anti-goat antibody solution (Rockland International), and then washed with a PBS + Tween solution. Proteins were visualized on film (Amersham) by incubation with West Pico Working Solution (Pierce) for 5 min.

Silver Staining

Silver staining of polyacrylamide gels was performed according to published protocols (21).

Affinity Chromatography

Anti-fluorescein antibody columns were prepared from the AminoLink Plus Immobilization Kit (Pierce) according to manufacturer instructions using affinity-purified anti-fluorescein goat antibody (Rockland International). Columns were prepared according to manufacturer instructions. Cell lysate was diluted to a final concentration of 0.1% SDS, 10% Triton-X in PBS before loading onto the column. After loading, columns were washed with a solution of 1% Triton-X in PBS. Bound proteins were eluted with Pierce Elution Buffer.

Mass Spectrometry

Mass spectra obtained by MALDI-TOF MS were performed on a Voyager DePro mass spectrometer (Applied Biosystems) in the multi-user mass spectrometry laboratory at Caltech. Prior to analysis, protein samples were trypsin-digested (Promega) and

purified via Ziptip reverse-phase chromatography (Millipore). Mass spectra of proteins obtained by the Caltech Protein/Peptide Mass MicroAnalytical Laboratory (PPMAL) were trypsin-digested and the resulting peptides were analyzed by liquid chromatography/mass spectrometry on a API 365 triple quadropole/electrospray tandem mass spectrometer (Perkin Elmer/Sciex). Statistical significance of protein identification was determined by PPMAL using the Mowse scoring algorithm.

Ultrafiltration

Ultrafiltration was performed with Microcon ultrafiltration devices (Millipore) according to manufacturer instructions. In order to prevent protein loss on the device, the membrane was passivated using 1% milk in water. The device was subsequently washed with water, and water was centrifuged three times through, as per manufacturer instructions.

Inhibitory Conditions of Polyamide Uptake

Cells were grown, trypsinized, resuspended, plated, and incubated as above for determining the inhibition of uptake by polyamide conjugate **FITC-7-Dz**. After 24 h of growth, the media was removed and replaced with 150 μL of media containing the inhibitory drugs at the concentrations given. The cells were incubated for 30 min. Following this, 7.5 μL of either a **FITC-1** stock solution (100 μM), a tetramethylrhodamine-conjugated transferrin stock solution (21 μM; Molecular Probes), or a Hoechst 33342 stock solution (100 μM; Molecular Probes) was added to the cells and mixed by gentle pipeting up and down of the media. The cells were incubated an

additional 2.5 h or 4 h, followed by imaging on a 2-photon laser microscope. Uptake rescue experiments were conducted as previously described (4). Temperature-dependence studies were conducted as above, except normal, unmodified media was used and the cells were incubated at the temperature given.

References

1. Dervan, P.B., Poulin-Kerstien, A.T., Fechter, E.J., and Edelson, B.S. (2005) Regulation of gene expression by synthetic DNA-binding ligands. *Top. Curr. Chem.*, **253**, 1–31.

2. Dervan, P.B. and Edelson, B.S. (2003) Recognition of the DNA minor groove by pyrrole-imidazole polyamides. *Curr. Opin. Struct. Biol.*, **13**, 284–299.

3. Edelson, B.S., Best, T.P., Olenyuk, B., Nickols, N.G., Doss, R.M., Foister, S., Heckel, A., and Dervan, P.B. (2004) Influence of structural variation on nuclear localization of DNA-binding polyamide-fluorophore conjugates. *Nucleic Acids Res.*, **32**, 2802–2818.

4. Best, T.P., Edelson, B.S., Nickols, N.G., and Dervan, P.B. (2003) Nuclear localization of pyrrole-imidazole polyamide-fluorescein conjugates in cell culture. *Proc. Natl. Acad. Sci. U S A*, **100**, 12063–12068.

5. Belitsky, J.M., Leslie, S.J., Arora, P.S., Beerman, T.A., and Dervan, P.B. (2002) Cellular uptake of N-methylpyrrole/N-methylimidazole polyamide-dye conjugates. *Bioorg. Med. Chem.*, **10**, 3313–3318.

6. Crowley, K.S., Phillion, D.P., Woodard, S.S., Schweitzer, B.A., Singh, M., Shabany, H., Burnette, B., Hippenmeyer, P., Heitmeier, M., and Bashkin, J.K. (2003) Controlling the intracellular localization of fluorescent polyamide analogues in cultured cells. *Bioorg. Med. Chem. Lett.*, **13**, 1565–1570.

7. Nickols, N.G., Jacobs, C.S., Farkas, M.E., and Dervan, P.B. (2007) Improved nuclear localization of DNA-binding polyamides. *Nucleic Acids Res.*, **35**, 363–370.

8. Best, T.P., *unpublished results*.

9. Brunner, J. (1993) New photolabeling and crosslinking methods. *Annu. Rev. Biochem.*, **62**, 483–514.

10. Brunner, J., Senn, H., and Richards, F.M. (1980) 3-Trifluoromethyl-3-phenyldiazirine. A new carbene generating group for photolabeling reagents. *J. Biol. Chem.*, **255**, 3313–3318.

11. Baird, E.E. and Dervan, P.B. (1996) Solid phase synthesis of polyamides containing imidazole and pyrrole amino acids. *J. Am. Chem. Soc.*, **118**, 6141–6146.

12. Zhao, Y., Zhang, W., Kho, Y., and Zhao, Y. (2004) Proteomic analysis of integral plasma membrane proteins. *Anal. Chem.*, **76**, 1817–1823.

13. Schnell, J.R., Dyson, H.J., and Wright, P.E. (2004) Structure, dynamics, and catalytic function of dihydrofolate reductase. *Annu. Rev. Biophys. Biomol. Struct.*, **33**, 119–140.

14. Qian, Z.M., Li, H., Sun, H., and Ho, K. (2002) Targeted drug delivery via the transferrin receptor-mediated endocytosis pathway. *Pharmacol Rev.*, **54**, 561–587.

15. Rejman, J., Bragonzi, A., and Conese, M. (2005) Role of clathrin- and caveolae-mediated endocytosis in gene transfer mediated by lipo- and polyplexes. *Mol. Ther.*, **12**, 468–474.

16. Watson, P., Jones, A.T., and Stephens, D.J. (2005) Intracellular trafficking pathways and drug delivery: fluorescence imaging of living and fixed cells. *Adv. Drug Deliv. Rev.*, **57**, 43–61.

17. Suzuki, T., Futaki, S., Niwa, M., Tanaka, S., Ueda, K., and Sugiura, Y. (2002) Possible existence of common internalization mechanisms among arginine-rich peptides. *J. Biol. Chem.*, **277**, 2437–2443.

18. Jiang, B.H., Semenza, G.L., Bauer, C., and Marti, H.H. (1996) Hypoxia-inducible factor 1 levels vary exponentially over a physiologically relevant range of O2 tension. *Am. J. Physiol.*, **271**, C1172–1180.

19. Hariton-Gazal, E., Rosenbluh, J., Graessmann, A., Gilon, C., and Loyter, A. (2003) Direct translocation of histone molecules across cell membranes. *J. Cell. Sci.*, **116**, 4577–4586.

20. Lalande, M.E., Ling, V., and Miller, R.G. (1981) Hoechst 33342 dye uptake as a probe of membrane permeability changes in mammalian cells. *Proc. Natl. Acad. Sci. U S A*, **78**, 363–367.

21. Shevchenko, A., Wilm, M., Vorm, O., and Mann, M. (1996) Mass spectrometric sequencing of proteins silver-stained polyacrylamide gels. *Anal. Chem.*, **68**, 850–858.